Ingeniería e Investigación
ISSN: 0120-5609
revii_bog@unal.edu.co
Universidad Nacional de Colombia
Colombia

Moreno Téllez, Carlos Mauricio; Sánchez, José Manuel; Higuera Cobos, Oscar Fabián
Characterising -AlTiN coating and assessing its performance during Ti-6Al-4V milling
Ingeniería e Investigación, vol. 33, núm. 2, agosto, 2013, pp. 9-15
Universidad Nacional de Colombia
Bogotá, Colombia

Characterising µ-AlTiN coating and assessing its performance during Ti-6Al-4V milling

Caracterización y desempeño del recubrimiento µ-AlTiN durante el fresado del Ti-6Al-4V

C. M. Moreno Téllez[1], J. M. Sánchez[2] and O. F. Higuera Cobos[3]

ABSTRACT

This study investigated the mechanical properties and performance of µ-AlTiN coating deposited by PVD cathodic arc technique for a specific Al0, 67Ti0, 33N composition deposited on a WC-Co and AISI D2 steel substrate. The structure of the coating was analysed using SEM, EDAX, XRD, AFM and TEM. Nano indentation measurements were used for analysing mechanical properties; the coating's performance was evaluated during the milling of a titanium alloy (Ti6Al4V). The TiN film was initially deposited to improve adhesion between coating and substrate, where columnar grains ranging in size from 200 to 500 nm were observed having NaCl-type structure. µ-AlTiN grain growth was also columnar but had ~50 nm grain size. The µ-AlTiN coated tool life was compared to an uncoated tool to determine the coating's influence during Ti6Al4V milling. The µ-AlTiN coating improved tool life by 100% compared to that of an uncoated tool due to aluminium oxide and TiC formation on the surface and a decrease in friction coefficient between the chip and the tool.

Keywords: AlTiN coating, cathodic arc deposition, milling, Ti6Al4V alloy.

RESUMEN

Las propiedades mecánicas y el desempeño del recubrimiento µ-AlTiN depositado por la técnica PVD por arco catódico ha sido investigada para una composición específica de Al0,67Ti0,33N depositada en sustrato de WC-Co y acero AISI D2; su estructura fue analizada usando SEM, EDAX, DRX, AFM y TEM, y las propiedades mecánicas se analizaron a partir de medidas de nanoindentación. El desempeño del recubrimiento fue evaluado durante el fresado de una aleación de titanio (Ti6Al4V). Una película de TiN fue depositada inicialmente para aumentar la adhesión del recubrimiento con el sustrato, donde se observan granos columnares entre 200 y 500 nm de estructura tipo NaCl y crecimiento de granos del µ-AlTiN también columnares con tamaño de grano ~50 nm. La vida de la herramienta recubierta fue comparada con otra sin recubrir para determinar la influencia del recubrimiento durante el fresado del Ti6Al4V. El recubrimiento µ-AlTiN mejora la vida de la herramienta en un 100% respecto a la herramienta sin recubrir, debido a la formación de un óxido de aluminio y TiC en la superficie y en la disminución del coeficiente de fricción entre el chip y la herramienta.

Palabras clave: AlTiN, depósito por arco, fresado, aleación Ti6Al4V.

Received: June 6th 2012
Accepted: June 5th 2013

Introduction

Wear-resistant coatings for machining application of aerospace alloys (including titanium alloys) are being continuously developed. Coatings such as TiN have been used successfully in milling this type of alloy due to the coating's advantages, including excellent substrate adhesion, low chemical reactivity, high temperature resistance, high hardness to reduce wear and low friction coefficient (Horling, 2002; Suresha, 2006); however, the working temperature limits its properties. Studies have been carried out to avoid such limitation, based mainly on adding aluminium to this compound (Knotek *et al.*, 1986; Jehn, 1986). It has been found that the compound formed (titanium aluminum nitride - Ti1-xAlxN) has greater oxidation resistance, allowing higher cutting speeds during machining, prolonging tool life by enabling the machining of hard materials and thereby lowering manufacturing costs (Fox-Rabinovich, 2010; Horling, 2002; PalDey *et al.*, 2004)

The mechanism responsible for excellent performance during cutting with Ti1-xAlxN coating is associated with the aluminium content as greater resistance to oxidation will be noticed with higher aluminium content in Ti1-xAlxN (Knotek *et al.*, 1986; Kim, 1999; Sjolen, 2007). For example, TiN is oxidised at temperatures ranging from 500 to 600°C, whereas Ti1-xAlxN oxidation begins at 750 to 900°C (McIntyre, 1990) so that such coatings

[1] Carlos Mauricio Moreno Téllez. Doctor en Materiales, Universidad de Navarra, España. Affiliation: Universidad Pedagógica y Tecnológica de Colombia - UPTC, Colombia. E-mail: carlosmauricio.moreno@uptc.edu.co
[2] José Manuel Sánchez. Doctor en Física, Universidad de Navarra, España. Affiliation: Centro de Estudios e Investigaciones Técnicas de Guipúzcoa and Universidad de Navarra, España. E-mail: jmsanchez@ceit.es
[3] Oscar Fabián Higuera Cobos. Magister en Ingeniería Metalúrgica, Universidad Industrial de Santander, Colombia. Candidato a Doctor en Ciencia e Ingeniería de los Materiales, Universidad Politécnica de Cataluña, España. Affiliation: Universidad Tecnológica de Pereira - UPTC, Colombia. E-mail: osfahico@utp.edu.co

How to cite: Moreno, C. M., Sánchez, J. M., Higuera, O. F., Characterising µ-AlTin coating and assessing its performance during Ti-6Al-4V milling., Ingeniería e Investigación. Vol. 33, No. 2. August 2013, pp. 9 – 15.

can be used at higher temperatures, ranging from 750 to 800°C (McIntyre, 1990). Some authors claim that Ti, Al, N hardness depends on Al content in the coating, reaching its maximum value at 50% Al concentration. However, the properties fall dramatically when content is more than 50% Al due to the formation of the "wurtzite" hexagonal phase (Zhou, 1999). Another factor to take into account, regardless of the coating, is that coatings deposited by physical vapour deposition (PVD) are characterised by significant surface roughness, mainly due to the formation of "droplets" which are deposited on substrate surface. There are different techniques to remove and eliminate the droplets. Coatings treated by such techniques are called microstructured coatings. The effect of removing droplets results in a decreased friction coefficient between the chip and the tool, thereby improving cutting performance by using aluminum titanium nitride (μ-AlTiN).

The main problem concerning characterising the coating is the influence of the substrate on measurements, primarily in nanoindentation assays and in X-ray diffraction tests. Models have been used to correctly predict both hardness values and eliminate or avoid this influence, i.e. Young's modulus for nanoindentation tests (Korsunsky, 1998; King, 1987). An alternative grazing angle technique has been used for X-ray diffraction. This study was thus aimed at exploring the microstructure and mechanical properties of an μ-AlTiN coating deposited by PVD cathodic arc technique and determining performance during titanium alloy (Ti6Al4V) milling.

Experimental procedure

The μ-Al0.67Ti0.33N coating was deposited on a WC-Co and AISI D2 steel substrate using the cathodic arc technique. The substrates were polished using 1 μm diamond paste and thoroughly cleaned. The coating was deposited using PLATIT PL50 and PLATIT PL1.000 reference machines in the following conditions: 430°C, 10^{-2} to 5.10^{-2} mbar pressure, 200 amp cathode current at 80 V. The samples were placed in a rotating system having variable speed. Coating thickness was measured using a Calotest assay and adherence to the substrate was determined using VDI 3198 standard procedure (Verein Deutscher Ingenieure Normen, 1991).

The X-ray diffraction (XRD) technique was used for identifying coating phases with Cu Kα glancing angle radiation and ω = 3 ° constant incidence angle using an optical parallel beam regarding incident beam and a crossed-slit collimator and graphite monochromator concerning the diffracted beam. Residual stresses were obtained from a graphical system SSFX (Perry *et al*., 1999). Hardness and elastic modulus were measured by nanoindentation technique (Berkovich) on a Nano Indenter II (MTS, Oak Ridge, TN).

Hardness and elastic modulus values were obtained from load compared to displacement curves using the method proposed by Oliver and Pharr (Oliver, 1992) and normalised with Korsunsky and King models to eliminate substrate effect (Korsunsky, 1998; King, 1987). Young's modulus was used to calculate residual stresses from XRD data. The μ-Al0.67Ti0.33N coating was examined by transmission electron microscopy (TEM) using a JEOL JEM 2100 microscope, operated at 200 kV at 2.3 Å resolution. The milling tests were carried out using K25 grade, 8-toothed, cemented carbide integral tools and 20 mm Φ. A 3-axis Kondia B500P machine was used for machining a 30 X 300 X160 mm titanium grade 5 (Ti-6Al-4V) alloy plate, annealed at 750°C for 2h.

Machining tests were carried out at 100 m / min cutting speed, 0.5 mm cutting depth, 70% of the total diameter being in contact with the titanium plate. Feed per tooth was 0.04 mm which gave 728 mm / min advance. A LEICA microscope was used for measuring the wear on the edge of the tool. The flank and rake face of the cutting edges were carefully inspected by SEM after flank wear reached around 0.25 mm.

Results and analysis

Microstructural analysis

Figure 1 shows the difference in surface roughness between the AlTiN coating without removal of droplet treatment and the μ-AlTiN treated surface. It was observed that the droplets had been completely eliminated. Values obtained from the AFM technique indicated that the coating's surface roughness changed from ~ 120 nm for AlTiN to ~ 30 nm for μ-AlTiN.

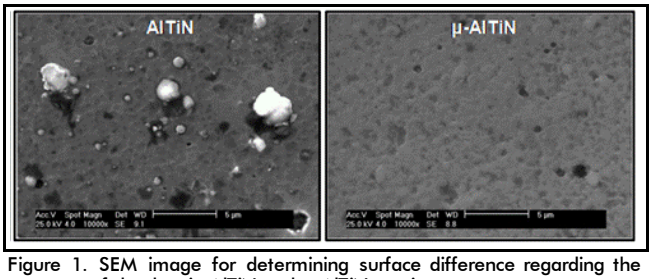

Figure 1. SEM image for determining surface difference regarding the presence of droplets in AlTiN and μ-AlTiN coatings

As expected, μ-AlTiN coating mechanical properties were exactly the same as those for AlTiN. However, eliminating surface defects provided greater stability on the edges of the tool during machining. Removing the droplets contributed towards reducing the friction coefficient generated between the chip and the tool, as described above.

Figure 2 (a) shows a TEM image of the cross-section of the μ-AlTiN coating deposited on WC-Co. An initial TiN film area can be observed having NaCl B1cubic structure which was aimed at increasing coating adhesion to the substrate (Gredic *et al*., 1991; Navinsek *et al*., 2001). Columnar grain growth can be noticed, as often reported concerning PVD-obtained coatings. The columnar grains were 0.2 - 0.5 μm at 1 μm film thickness. The grains adopted a TiN-like structure when Al was added; however, grain size decreased considerably to around 50nm, as can be seen in Figure 2 (b). The compound μ-AlTiN resulted from replacing Ti atoms by Al atoms in the TiN crystalline structure. The coatings' lattice parameter thus gradually decreased from 4.25 to 4.19 Å when Al content increased, as the atomic size of Al is smaller than that for Ti.

The remarkable decrease in μ-AlTiN grain size had a considerable influence on this coating's mechanical properties. Figure 3 (a) shows bands which corresponded to the transition between TiN and μ-AlTiN. The dark bands were TiN coating and the light bands the μ-AlTiN coating. The diffraction patterns obtained for the μ-AlTiN coating are shown in Figure 3 (b). FCC structure planes can be seen. The XRD values led to concluding that the μ-AlTiN coating had a strong preferred orientation in the plane (200) which, according to Pelleg *et al*., (Pelleg, 1991) represent the lower surface energy planes following deposition. The current phases corresponded to NaCl cubic crystal structure systems (see Figure 4).

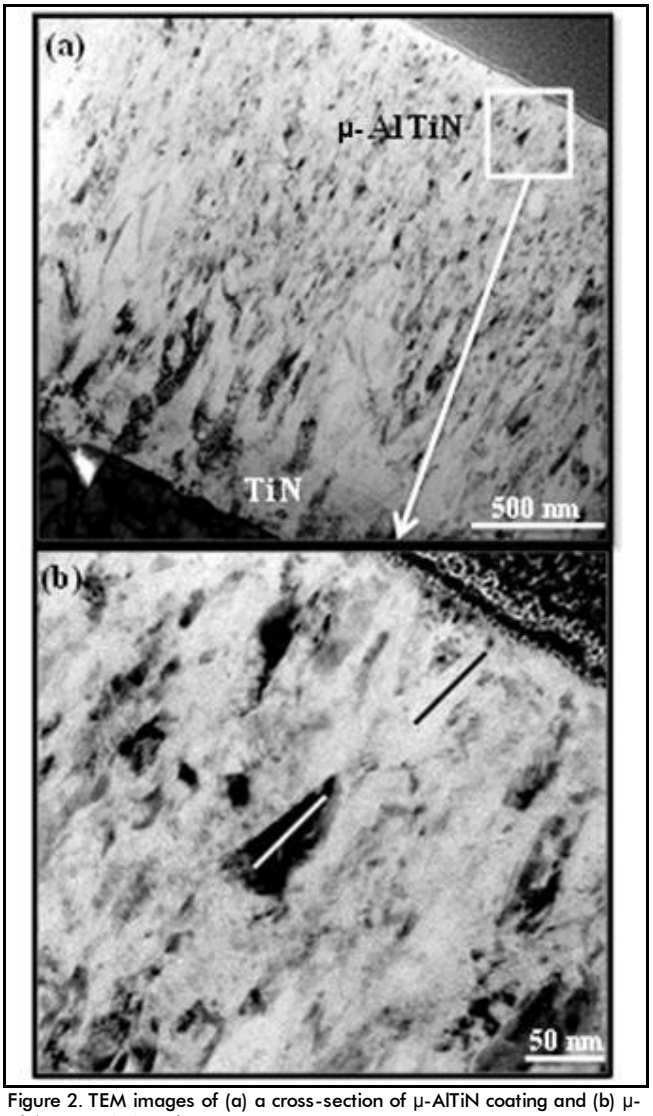

Figure 2. TEM images of (a) a cross-section of μ-AlTiN coating and (b) μ-AlTiN on WC-Co substrate

Mechanical and tribological properties

The indentation depth should be maintained within 10% of the film's total thickness regarding hardness and as a general rule (Horling, 2002). However, certain models have attempted a more precise quantification of substrate influence on measurements of hardness and Young's modulus. Korsunsky (Korsunsky, 1998) and King (King, 1987) each developed a mathematical model for the general analysis of indentation in a substrate-coating system which led to determining coating hardness and Young's modulus, eliminating the effect of the substrate. Figure 5 (a) shows the hardness values at different indentation depths and curve fit from Korsunsky's model (Korsunsky, 1998), where y-axis value was hardness calculated with the model and β the relative indentation depth, defined as the ratio between maximum penetration depth and coating thickness. Figure 5 (b) shows Young modulus values for μ-AlTiN coating on different substrates, WC-Co and AISI D2 steel adjusted from King's modified model (Saha et al., 2002) where a was the square root of the projected contact area, t film thickness and α the model's adjustment parameter.

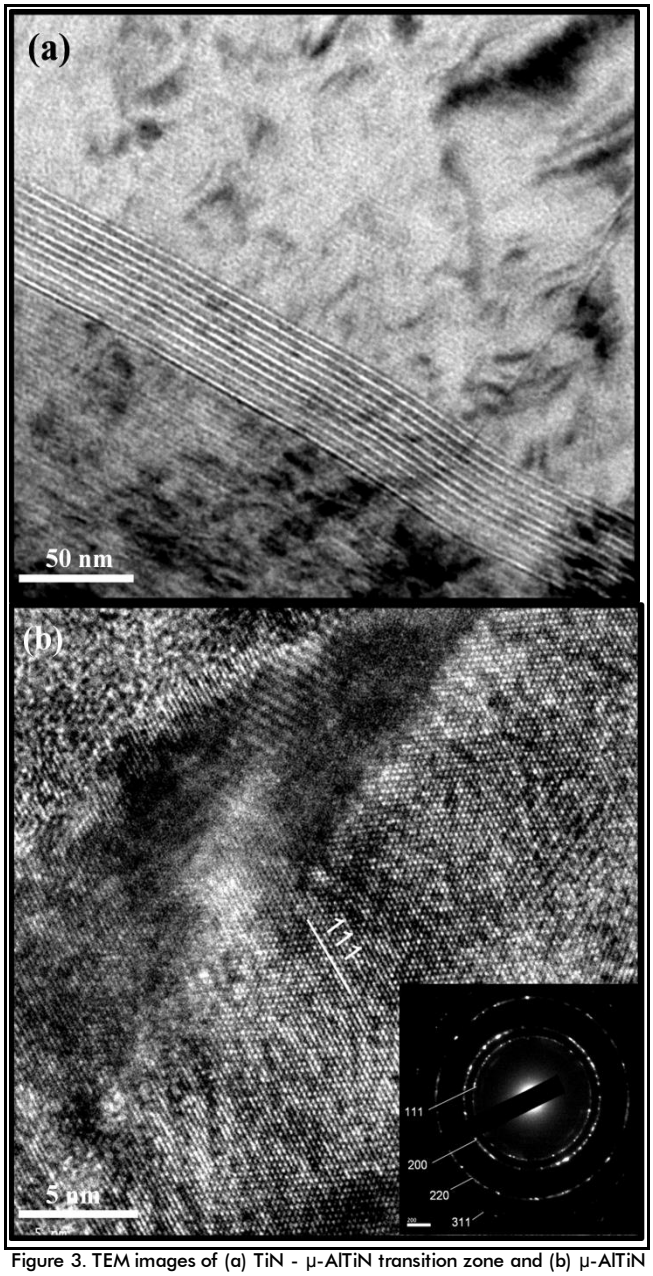

Figure 3. TEM images of (a) TiN - μ-AlTiN transition zone and (b) μ-AlTiN on WC-Co substrate and its corresponding diffraction pattern

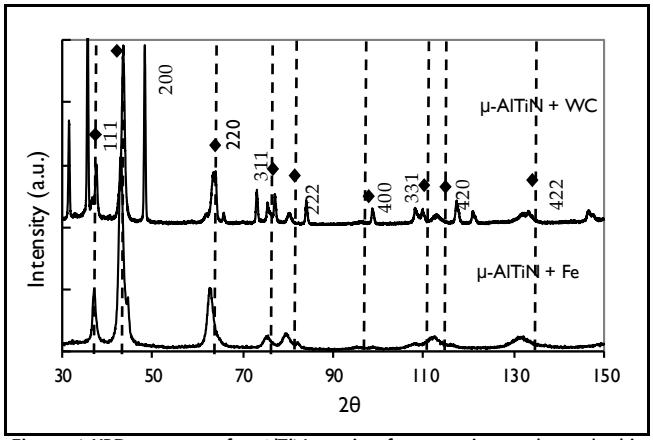

Figure 4 XRD patterns of μ-AlTiN coating from grazing angle method in WC-Co and steel substrates

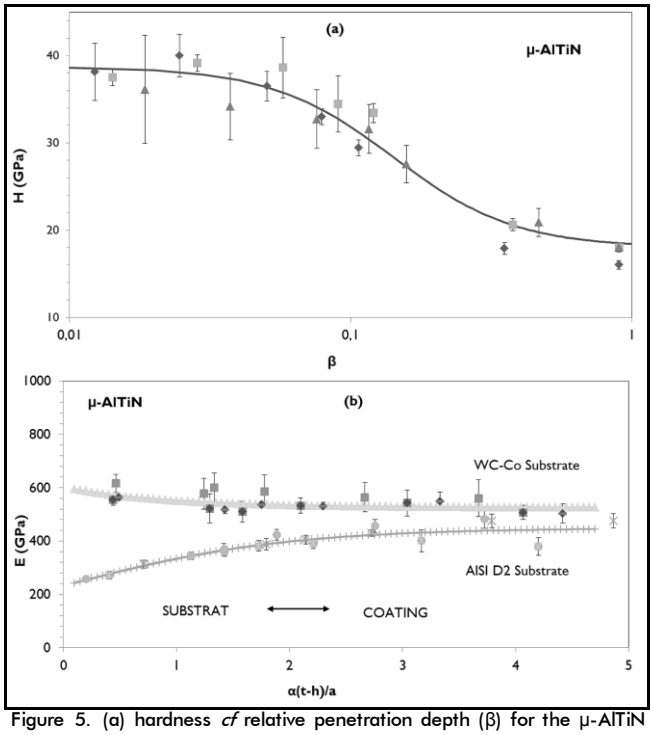

Figure 5. (a) hardness *cf* relative penetration depth (β) for the μ-AlTiN coating on WC-Co substrate for different thicknesses, adjusted with Korsunsky's model (Korsunsky, 1998) and (b) comparison of Young's modulus fof the μ-AlTiN coating on AISI D2 steel and WC-Co substrate, adjusted with King's modified model (Saha *et al.*, 2002).

Table 1 shows hardness and Young's modulus values calculated for TiN and μ-AlTiN coatings deposited on WC-Co. The first conclusion was that coating hardness did not depend on coating thickness, this being consistent with the PVD cathodic arc deposit method where ions deposited by this method are constant and the layers so formed are homogeneous because of good control over the method (Curtins, 1995). μ-AlTiN coating had a higher hardness value compared to TiN hardness.

Table 1. Hardness and Young's modulus for TiN and μ-AlTiN coatings deposited on hard metal samples

Coating	Thickness (μm)	Hardness (GPa)	Young's modulus (GPa)
TiN	1,6-3,6	33±0,6	540±35
μ-$Al_{0.67}Ti_{0.33}N$	1,7-3	38±0,6	485±40

Increased μ-AlTiN coating hardness could be explained by the decreased interatomic distance resulting from adding Al, this being associated with increased Ti1-xAlxN system covalent energy (PalDey *et al.*, 2003). Young's modulus for the μ-AlTiN coating was lower than the modulus calculated for TiN coating. This combination of hardness and Young's modulus made the μ-AlTiN coating into a hard but not particularly rigid material which might lead to good performance against wear (Wang, 2013; Aihua, 2012).

Residual stress

Residual stress values for the coatings on AISI D2 steel and WC-Co substrate were calculated by Sin2ψ (2θ = 130° with Cr radiation) and grazing angle method (Cu radiation). The glancing angle method was used when coating peaks overlapped with substrate peaks, this being the usual case for WC-Co substrate. The stress values were calculated from elastic modulus values obtained by nanoindentation. Table 2 shows the residual stresses measured for the two coatings on AISI D2 steel substrate using the Sin2ψ method. The negative stress values indicated that they were compressive. The TiN coating had the lowest residual stress values, ~ -4.5 GPa, whereas the residual stress values for μ-AlTiN were ~ -6.7 GPa. The measured value for stress-free lattice TiN was 0.4245 nm ± 0.0001 nm, this being slightly larger (~ 0.1%) than the 0.4241 nm reference value (Wong-Ng, 1987).

Table 2. Residual stresses in the TiN and μ-AlTiN coatings deposited on AISI D2 steel samples using Sin2ψ

Coating	Residual stresses sen2ψ (MPa)	Stress-free lattice (nm)
TiN	-4400±200	0,4245
	-4400±200	0,4245
	-4600±250	0,4245
μ-$Al_{0.67}Ti_{0.33}N$	-6800±500	0,4170
	-6700±250	0,4173
	-6900±200	0,4174

As mentioned above, the problem of overlapping peaks in the hard metal substrate prevented the appearance of a coating peak from which the residual stress could be measured; however, this was possible for TiN (Table 3).

Table 3. Residual stresses for the TiN coating deposited on metal samples using the Sin2ψ method

Coating	Residual stresses, $sin^2\psi$ (MPa)	Stress-free lattice (nm)
TiN	-1800±200	0,4246
	-2200±200	0,4243
	-2500±250	0,4246

Residual stresses for TiN on WC-Co substrate were smaller than those for the AISI D2 steel substrate as the level of residual stress depended on the type of substrate: ~ -4.5 GPa for steel substrate and ~ -2, 2 GPa for the WC-Co substrate. The difference in stress values between substrates was due to the fact that residual stresses in the coating mainly had two contributions: thermal stresses due to the difference between the coating's thermal expansion coefficient and the substrate and inherent deposition stress (due to sputtering in the case of arc deposition):

$$\sigma_{residual} = \sigma_{th} + \sigma_{in} \qquad (1)$$

where: σ residual = total residual stresses, σ_{th} = thermal stresses and σ = inherent stresses. Considering constant the stresses of the substrate and the coating, one can determine the existing thermal stresses from the following expression:

$$\sigma_{th} = \frac{E_{coatings}}{1-\nu} \cdot \left(\alpha_{coating} - \alpha_{subst}\right)\left(T_{depo} - T_a\right) \qquad (2)$$

where $E_{coating}$ = Young's modulus for the coating, $\alpha_{coating}$ = the coating's thermal expansion coefficient, α_{subst} = the substrate's thermal expansion coefficient, T_{depo} = deposition temperature and Ta = room temperature. The substrates and coatings' thermal expansion coefficients were found in the literature (Wang, 1999). A constant inherent stress value for a coating was to be expected as the deposition conditions were the same. Total residual stress values of coatings deposited on WC-Co substrate obtained from grazing angle measurements are summarised in Table 4.

It was observed that the values obtained for TiN were in the same order of magnitude as those obtained by the Sin2ψ method; thereby validating the measurement method. The μ-AlTiN

coating deposited on different substrates was subject to large residual stresses ~ -7.0 GPa and had a 0.4172 ± 0.0003 nm lattice parameter.

Table 4. Residual stresses for TiN and μ-AlTiN coatings deposited on hard metal samples by the glancing angle method

Coating	Young's modulus (GPa)	Residual stress glancing angle (MPa)	Stress-free lattice (nm)
		-1,500	0.4241
TiN	540±35	-2,600	0.4241
		-2,700	0.4243
		-6,700	0.4174
μ-$Al_{0.67}Ti_{0.33}N$	485±40	-6,400	0.4171
		-6,900	0.4171

It was observed that the values obtained for TiN were in the same order of magnitude as those obtained by the Sin2ψ method; thereby validating the measurement method. The μ-AlTiN coating deposited on different substrates was subject to large residual stresses ~ -7.0 GPa and had a 0.4172 ± 0.0003 nm lattice parameter.

Wear testing

High speed milling (HSM) tests involved uncoated and coated surfaces using TiN and μ-AlTiN hard metal tools. Figure 6 shows in detail the wear of an edge of an uncoated tool for a 30 m mechanised length. The wear zone was about 250 microns. The most important phenomenon was the built-up edge resulting from Ti6Al4V material adhering to the flank of the cutter blade (see Figure 6, zone 1). This type of wear accelerated chipping of the tool's cutting edges. Figure 6 (zone 2) shows the WC-Co substrate material, although there was evidence of some remnants of Ti6Al4V from EDAX analysis. Zone 3, Figure 6, whose dark colour contrasted with the rest, had similar composition to the previous one but with added oxygen and carbon (as results in the EDAX analysis), suggesting the formation of an aluminium oxide and TiC on the surface.

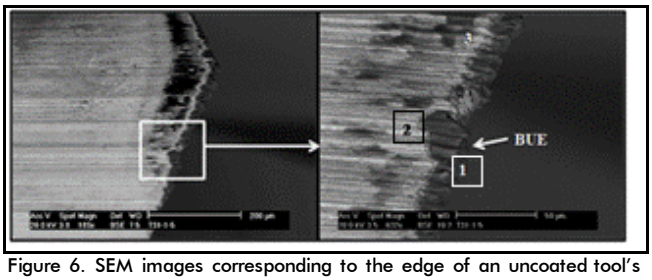

Figure 6. SEM images corresponding to the edge of an uncoated tool's blade after 20 m machining

It should be noted that this oxide was not observed on the edge but at a distance of around 20-30 microns. This could be explained considering that the edge was in contact with the material to be cut so that oxygen access was restricted. Coating oxidation occurred at the point where the cutting tool was no longer in contact with the machining material or its shavings (known as depth of cut notch - DOCN). The presence of aluminium oxide was confirmed from EDAX analysis. The presence of the coating was evidenced by an atomic Al / Ti ratio. Furthermore, values indicating a higher Al / Ti ratio and the presence of oxygen in the area adjacent to the cutting zone agreed with data reported in the literature which indicated that the μ-AlTiN coating produced an Al oxide film just in the region where the chip was separated from the edge of the tool (Horling, 2005). The formation of this oxide offered protection from the notch. The most plausible hypothesis for the aluminium oxide layer formation was that it was an oxidation product from the Al existing in the coating since the presence of this element in Ti6Al4V was very low. Figure 7, zone 3, shows the normal μ-AlTiN coating with oxygen still present but in a smaller proportion than in zone 2, according to EDAX results.

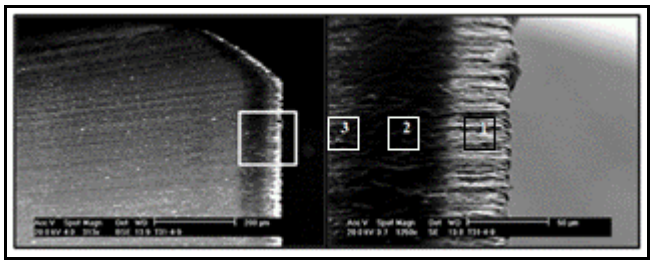

Figure 7. SEM images showing the edge flack of a μ-AlTiN-coated tool after 38 m machining

The uncoated tool's performance during HSM led to the conclusion that the presence of the built-up edge may have been causing chipping of cutting edges, eventually producing unstable cutting and decreasing the tool's lifetime. The adhesion caused by BUE may have been related to the large-scale chemical interaction between elements of the tool and the titanium alloy. Regarding the μ-AlTiN coated tool, and unlike the uncoated tool, it was noted that in Figure 7 (zone 1) the flank showed that edge linearity was maintained at 38m mechanised distance. EDAX analysis confirmed the presence of μ-AlTiN coating. The presence of an aluminium oxide was again detected in zone 2 , which appeared in dark contrast in SEM images (see Figure 7).

It should be noted that this oxide was not observed on the edge but at a distance of around 20-30 microns. This could be explained considering that the edge was in contact with the material to be cut so that oxygen access was restricted. Coating oxidation occurred at the point where the cutting tool was no longer in contact with the machining material or its shavings (known as depth of cut notch - DOCN). The presence of aluminium oxide was confirmed from EDAX analysis. The presence of the coating was evidenced by an atomic Al / Ti ratio. Furthermore, values indicating a higher Al / Ti ratio and the presence of oxygen in the area adjacent to the cutting zone agreed with data reported in the literature which indicated that the μ-AlTiN coating produced an Al oxide film just in the region where the chip was separated from the edge of the tool (Horling, 2005). The formation of this oxide offered protection from the notch. The most plausible hypothesis for the aluminium oxide layer formation was that it was an oxidation product from the Al existing in the coating since the presence of this element in Ti6Al4V was very low. Figure 7, zone 3, shows the normal μ-AlTiN coating with oxygen still present but in a smaller proportion than in zone 2, according to EDAX results.

It is well-known that aluminium oxide is a very stable ceramic compound which is normally used as a diffusion barrier in various machining tools. The μ-AlTiN coating thus has the advantage of producing this highly refractory layer during cutting by passive oxidation of the mixed nitride, besides acting as an effective and stable barrier against the diffusion and chemical interaction observed by studies reported in the pertinent literature (PalDey *et al*., 2003; Wang *et al*., 1988; Moreno *et al*., 2005). Figure 8 summarises the wear curves produced during machining, reflecting the coatings used and referring to the uncoated tool. The curves showed that μ-AlTiN coating was most suitable for face milling the Ti6Al4V alloy, leading to 100% performance improvement compared to the uncoated tool used today.

Given these results, tool wear can be described as a combination of the following:

1. Thermally-activated chemical interaction, associated with the reaction between the coating and the alloy Ti6Al4V;

2. Once the coating disappears, the hard metal substrate loses C which diffuses into the chip; this produces a strong bond between them which is the most likely cause of the formation of edge build-up;

3. The built-up edge is an irregularity strongly adhering to the cutting edge which can cause it to crack because of the torque applied by the passing of the chip; and

4. The final failure of tools is associated with the presence of these micro-fractures and depth of cut notch (DOCN). Such phenomenon is associated with the concentration of damage in this region due to the presence of high temperatures in contact with atmospheric oxygen.

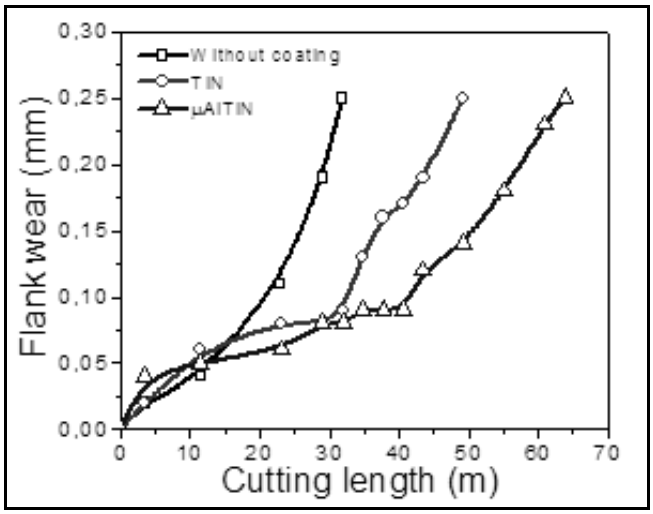

Figure 8. Curves for edge flank wear *cf* the length of the cutting of different coatings used for the HSM of Ti6Al4V

Conclusions

HSM tests showed that the µ-AlTiN coating had the best performance in machining Ti6Al4V alloy, mainly due to the combination of good mechanical properties (such as high hardness value and its Young's modulus) with high resistance to oxidation, primarily due to the formation of an aluminium oxide layer acting as a passivator and going against corrosion formation. It also had sufficient toughness to prevent premature fracture during cutting. Reduced surface roughness in this coating allowed further improvement in the tools' performance.

References

Aihua, L., et al., Friction and wear properties of TiN, TiAlN, AlTiN and CrAlN PVD nitride coatings., International Journal of Refractory Metals and Hard Materials, Vol. 31, 2012, p. 82-88.

Curtins, H., PLATIT: A new industrial approach to cathodic arc coating technology., Surface and Coatings Technology, Vol. 76-77 (Part 2), 1995, pp. 632-639.

Fox-Rabinovich, G. S., et al., Multi-functional nano-multilayered AlTiN/Cu PVD coating for machining of Inconel 718 superalloy., Surface and Coatings Technology, Vol. 204, No.15, 2010, pp. 2465-2471.

Horling, A., Thermal stability of arc evaporated high aluminum-content Ti1-xAlxN thin films., Journal of Vacuum Science & Technology a-Vacuum Surfaces and Films., Vol. 20, No. 5, 2002, pp. 1815-1823.

Gredic, T., Zlatanovic M., Plasma Deposition of (Ti,Al)N Coatings at Various Magnetron Discharge Power Levels., Surface & Coatings Technology, Vol. 48, No.1, 1991, pp. 25-30.

Horling, A., Mechanical properties and machining performance of Ti1-xAlxN-coated cutting tools., Surface and Coatings Technology, Vol. 191, No.2-3, 2005, pp. 384-392.

Horling, A., Thermal stability and mechanical properties of arc evaporated (Ti,Al)N thin films., Linköpings, Department of Physics and Measurement Technology, Linköpings Universitet, 2002, pp. 14-32.

Jehn, H. A., Morphology and Properties of Sputtered (Ti,Al)N Layers on High-Speed Steel Substrates as a Function of Deposition Temperature and Sputtering Atmosphere., Journal of Vacuum Science & Technology a-Vacuum Surfaces and Films, Vol. 4, No. 6, 1986, pp. 2701-2705.

Kim, B. J., High temperature oxidation of (Ti1-xAlx)N coatings made by plasma enhanced chemical vapor deposition., Journal of Vacuum Science & Technology a-Vacuum Surfaces and Films, Vol. 17, No.1, 1999, pp. 133-137.

King, R. B., Elastic Analysis of Some Punch Problems for a Layered Medium., International Journal of Solids and Structures, Vol. 23, No.12, 1987, pp. 1657-1664.

Knotek, O., Bohmer, M., Leyendecker, T., On Structure and Properties of Sputtered Ti and Al Based Hard Compound Films., Journal of Vacuum Science & Technology a-Vacuum Surfaces and Films, Vol. 4, No.6, 1986, pp. 2695-2700.

Korsunsky, A. M., On the hardness of coated systems., Surface and Coatings Technology, Vol. 99, No.1-2, 1998, pp. 171-183.

McIntyre, D., Oxidation of Metastable Single-Phase Polycrystalline Ti0.5al0.5n Films - Kinetics and Mechanisms., Journal of Applied Physics, Vol. 67, No.3, 1990, pp. 1542-1553.

Moreno, C.M., Artola, G., Sanchez, J.M., Interaction between Ti-6%Al-4%V alloys and hardmetals coated by cathodic-arc technology"., Functionally Graded Materials, Vol. VIII, 2005, pp. 353-358.

Navinsek, B., Panjan, P., Gorenjak, F., Improvement of hot forging manufacturing with PVD and DUPLEX coatings. Surface & Coatings Technology, Vol. 137, No.2-3, 2001, pp. 255-264.

Oliver, W. C., Pharr, G. M., An Improved Technique for Determining Hardness and Elastic-Modulus Using Load and Displacement Sensing Indentation Experiments. Journal of Materials Research, Vol. 7, No.6, 1992, pp. 1564-1583.

PalDey, S., Deevi, S. C., Alford, T.L., Cathodic arc deposited thin film coatings based on TiAlintermetallics., Intermetallics, Vol. 12, No.7-9, 2004, pp. 985-991.

PalDey, S., Deevi, S. C., Properties of single layer and gradient (Ti,Al)N coatings., Materials Science and Engineering A, Vol. 361, No.1-2, 2003, pp. 1-8.

PalDey, S., Deevi, S. C., Single layer and multilayer wear resistant coatings of (Ti,Al)N: a review., Materials Science and Engineering A, Vol. 342, No.1-2, 2003, pp. 58-79.

Pelleg, J., Zevin, L. Z., Lungo, S., Reactive-sputter-deposited TiN films on glass substrates. Thin Solid Films, Vol.197, 1991, pp.117-128.

Perry, A. J., Sue, J. A., Martin, P. J., Practical measurement of the residual stress in coatings. Surface and Coatings Technology, Vol. 81, No.1, 1996, pp. 17-28.

Saha, R., Nix, W. D., Effects of the substrate on the determination of thin film mechanical properties by nanoindentation., Acta Materialia, Vol. 50, No.1, 2002, pp. 23-38.

Sjolen, J., Structure and mechanical properties of arc evaporated Ti-Al-O-N thin films., Surface and Coatings Technology, Vol. 201, No.14, 2007, pp. 6392-6403.

Suresha, S. J., Processing, microstructure and hardness of TiN/(Ti, Al)N multilayer coatings., Materials Science and Engineering A,

Vol. 429, No.1-2, 2006, pp. 252-260.

Verein Deutscher Ingenieure Normen., VDI-Verlag, Dusseldorf, 1991, pp. 1-8

Wang, D. Y., Improvement of the interfacial integrity of (Ti,Al)N hard coatings deposited on high speed steel cutting tools., Surface and Coatings Technology, Vol.120-121, 1999, pp. 388-394.

Wang, M., Zhang Y.Z., Diffusion Wear in Milling Titanium-Alloys., Materials Science and Technology, Vol.4, No.6, 1988, pp. 548-553.

Wang, X., et al., Friction coefficient and sliding wear of AlTiN coating under various lubrication conditions., Wear, 2013. 304(1–2): p. 67-76.

Wong-Ng, W., Standard X-Ray Diffraction Powder Patterns of Sixteen Ceramic Phases., Powder Diffraction, Vol. 2, 1987, pp.54.

Zhou, M., Phase transition and properties of Ti-Al-N thin films prepared by rf-plasma assisted magnetron sputtering., Thin Solid Films, Vol. 339, No.1-2, 1999, pp. 203-208.